Chinese Chemical Letters 34 (2023) 107938

Contents lists available at ScienceDirect

Chinese Chemical Letters

journal homepage: www.elsevier.com/locate/cclet

Mass spectrometry profiling of single bacterial cells reveals metabolic regulation during antibiotics induced bacterial filamentation

Dongxue Zhang[a], Qin Qin[b], Liang Qiao[a,*]

[a] Department of Chemistry, Institutes of Biomedical Sciences, and Shanghai Stomatological Hospital, Fudan University, Shanghai 200000, China
[b] Changhai Hospital, The Naval Military Medical University, Shanghai 200433, China

ARTICLE INFO

Article history:
Received 2 July 2022
Revised 8 October 2022
Accepted 20 October 2022
Available online 23 October 2022

Keywords:
ESI-MS
Single bacterial cell analysis
Metabolome
Bacterial antimicrobial resistance
Bacterial filamentation

ABSTRACT

Bacterial antimicrobial resistance (AMR) is a severe threat to global health and development. Under the stimulation of antibiotics, bacterial cells can undergo filamentation and generate daughter cells with stronger AMR. The current research on bacterial AMR mechanism is mainly conducted with a population of cells. However, bacterial cells exhibit heteroresistance, making the study at population level not reliable. Herein, we developed single bacterial cell metabolic profiling by mass spectrometry (MS) to study bacterial AMR at single-cell level. By utilizing a microprobe controlled by a microoperation platform, single filamentous extended spectrum beta-lactamase (ESBL) producing *Escherichia coli* (ESBL-*E. coli*) cells generated by ceftriaxone sodium stimulation can be extracted and spray-ionized for MS analysis. Heterogeneous among ESBL-*E. coli* cells under the same antibiotic stimulus condition was observed from mass spectra as well as cell morphology. The metabolic profiles by MS of different individual cells can be clustered into subgroups well in accordance with bacterial cell length. Metabolic pathways including arginine and proline metabolism, as well as cysteine and methionine metabolism were disclosed to play an important role in the bacterial SOS-associated filamentation against antibiotics. The microprobe electrospray ionization-MS-based single bacterial cell analysis method is promising in the study of various bacterial AMR mechanism and can reveal the heterogeneity of bacterial AMR from-cell-to-cell.

Bacterial antimicrobial resistance (AMR) is an emerging serious problem threatening public health. The minimum number of infections caused by drug-resistant bacteria annually in the United States (U.S.) increased from 2 million in 2013 to 2.8 million in 2019 [1,2]. Extended spectrum beta-lactamase (ESBL) producing bacteria are one of the common antibiotic-resistant bacteria known as superbugs that synthesize enzymes to protect themselves against a number of beta-lactam antibiotics. ESBL-producing *Enterobacterales* caused 197,400 estimated cases in hospitalized patients and 9100 estimated deaths in 2017 in the U.S. [2]. The rapid development of bacterial AMR has called the urgent demand of developing new antibiotic drugs [3]. Studying the mechanism of bacterial AMR can provide theoretical basis for the development of new bacterial inhibition methods. To data, the current research on bacterial AMR mechanism is mainly performed with a population of cells [4,5]. However, bacterial cells are highly heterogeneous and usually display different resistance to antibiotics even when they are from the same microbial community and the same strain [6], making the bacterial AMR study at the population level not reliable.

Bacterial cells can generate SOS responses to defend against antibiotic drugs. Morphological change is one of the SOS responses [7]. Justice *et al.* reported that bacterial filamentation occurs when bacteria are exposed to beta-lactam antibiotics, and bacterial cells can survive until the antibiotics are diluted or inactivated [8]. Bos *et al.* found that *E. coli* cells can change their shape into filaments under the perturbation of sub-minimum inhibitory concentration (MIC) of ciprofloxacin, and the elongated bacterial cells can produce daughter cells with stronger AMR [9]. Banerjee *et al.* discovered that bacterial morphological changes can reduce the bacterial uptake of antibiotics and is a feedback strategy for bacteria to adapt to stressful environments [10]. In our previous work, we have combined matrix-assisted laser desorption/ionization time-of-flight mass spectrometry (MALDI-TOF MS) and gradient microfluidics to study the morphological changes of various bacteria under the impact of antibiotics and the corresponding protein expression changes. We observed that different individual cells can show distinctive morphological changes under the same antibiotic impaction environment. To better understand the bacterial AMR generated from the bacterial SOS responses, it is necessary to

* Corresponding author.
E-mail address: liang_qiao@fudan.edu.cn (L. Qiao).

https://doi.org/10.1016/j.cclet.2022.107938
1001-8417/

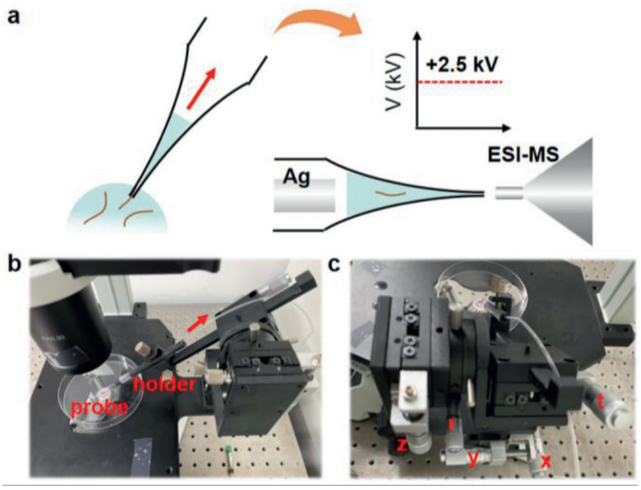

Fig. 1. (a) Schematic illustration of single bacterial cell analysis by probe ESI-MS. (b) A single bacterial cell pneumatic extraction by a microprobe under the control of a microoperation platform. (c) Five axes (x, y, z, r, t) of the microoperation platform (r: angle, t: microprobe direction).

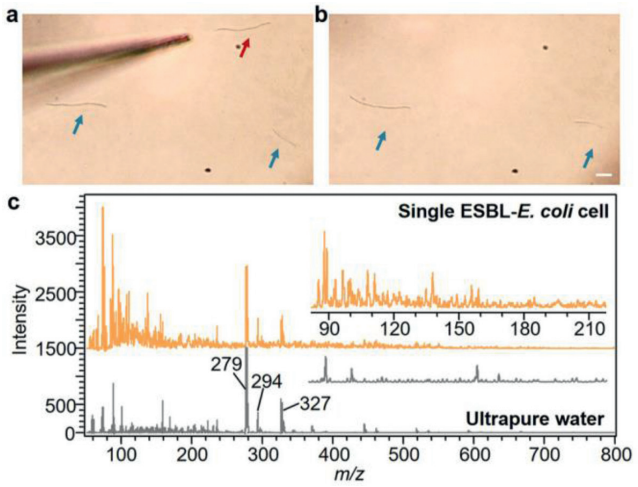

Fig. 2. A single ESBL-*E. coli* cell extracted by a microprobe: (a) before extraction, (b) after extraction (red arow: target cell; blue arrow: other cells; scale bar: 10 μm). (c) Mass spectra of a single ESBL-*E. coli* cell and ultrapure water.

characterize the *in-vivo* metabolic changes of the bacterial cells at single-cell level.

Techniques, such as microscopy, flow cytometry, and single cell PCR, have been widely used to study cells at single-cell level [11], and can be integrated with microfluidics to achieve high-throughput analysis and to reduce experimental operations [12,13]. However, these techniques are based on the knowledge of target molecules. In contrast, mass spectrometry (MS) can realize non-targeted molecular analysis for the discovery of new biomarkers. In the past few years, MS-based methods, such as mass-cytometry [14], capillary electrophoresis-trapped ion mobility MS [15], capillary dielectric barrier discharge ionization MS [16], have been developed for single-cell analysis [17]. Among various MS-based single cell analysis methods, probe electrospray ionization (ESI)-MS is most often used for single cell metabolic profiling, with the advantages of improved detection sensitivity, reduced interference to metabolite distribution during sampling, and simplified equipment [18]. Since the initial work by Gong *et al.* [18], a variety of single-cell analysis based on probe ESI-MS have been developed at cellular [19,20] and subcellular [21,22] level. Despite the rapid development of single cell MS analysis, there are few studies on single bacterial cell analysis by MS to date. Zhang *et al.* utilized the nanopore effect to measure bacterial cell size and further achieved bacterial identification by combining the nanopore effect and the mass spectrometry analysis [23].

In this study, we developed single bacterial cell profiling by MS to study the metabolic regulation during antibiotics-induced bacterial filamentation. The single bacterial cell MS analysis was performed with a microprobe ESI-MS method, as illustrated in Fig. 1a. Under the control of a microoperation platform, a single filamentous ESBL-producing *Escherichia coli* (ESBL-*E. coli*) cell generated under antibiotic stimulation was pneumatically extracted into a microprobe with the tip size of 3∼5 μm inner diameter (Figs. 1b and c, Fig. S1 in Supporting information). Then, an Ag wire was inserted into the microprobe from the rear to initiate ESI of the whole bacterial cell under the application of a direct current (DC) high voltage, which can assist in cell lysis and ionization [14,24]. The analysis of single bacterial cell by mass spectrometry was performed immediately after the cell extraction to avoid any changes compared to the observed cell morphology. The Ag wire was placed close to but not in contact with the sample to reduce dead volume, as well as to avoid surface adsorption of molecules and hence sensitivity loss [25]. To study the stability and reproducibility of the microprobe ESI-MS method, we collected 24 mass spectra of bacterial intracellular metabolites (Fig. S2 in Supporting information) and calculate the cosine correlation distribution between any two mass spectra. The bacterial intracellular metabolites were extracted from a population of bacterial cells as detailed in supporting information experimental section. All the cosine correlation was larger than 0.9 and the median was larger than 0.97 (Fig. S3 in Supporting information), demonstrating a high stability and reproducibility of the analysis platform. We used the bacterial intracellular metabolites as a benchmark sample because it was highly similar to the analytes of single-cell MS analysis and can avoid the cell-to-cell heterogeneity for reproducibility evaluation.

A single filamentous bacterial cell was extracted by a microprobe under the observation of an optical microscope, as shown in Figs. 2a and b. By comparing the mass spectra of the single bacterial cell to the background from ultrapure water, mass spectral peaks specific to the ESBL-*E. coli* cell could be detected as shown in Fig. 2c. The peaks specific to the ESBL-*E. coli* cell were mainly located within the *m/z* range of 100–200, which could be attributed to intracellular metabolites. The result demonstrated that the microprobe ESI-MS-based method can detect metabolites from a single bacterial cell. There were also intensive peaks (*m/z* 279, 294, 327 *etc.*) observed from the background of ultrapure water, which could be contaminants from atmosphere and in the operation system. For example, the peak at $m/z = 279$ could be the plasticizer dibutylphthalate according to previous publication [26].

In order to study the metabolic change during bacterial filamentation, we analyzed single ESBL-*E. coli* cells cultured with CEF for 2 h (2 h group) and 5 h (5 h group) by the microprobe ESI-MS. Mass spectra (*m/z* 50–800) of single elongated cells were recorded (Fig. S4 in Supporting information). Features were extracted from the raw MS data. Statistical analyses, including PCA (Fig. 3a) and cluster analysis (Fig. 3b), were performed on the extracted features. Normalization was performed by the sum of all the features. It was found that the mass spectral features from the 2 h and the 5 h groups could be well clustered into two discriminative groups, indicating that the metabolic status was significantly changed during bacterial elongation under the antibiotic stimulation. According to volcano plot, 123 features with significant regulation (fold change > 1.5 or < 0.66 and P-value < 0.05) were found between the 2 h group and the 5 h group (Fig. 3c).

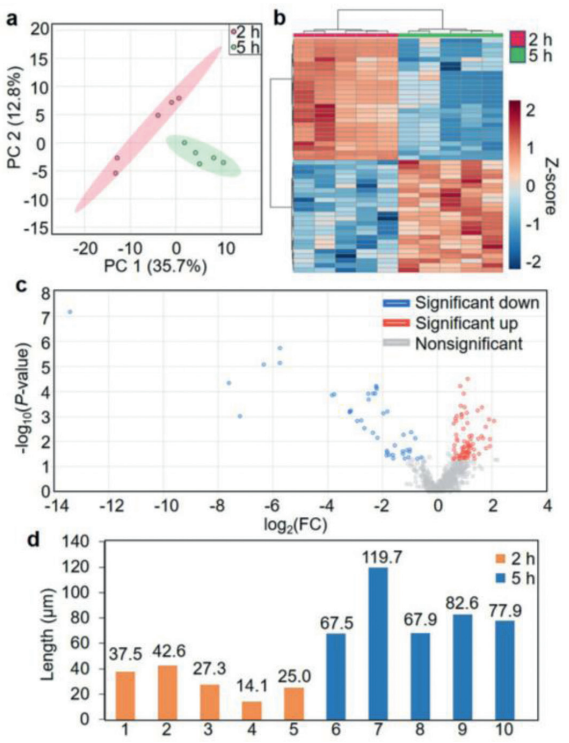

Fig. 3. (a) PCA, (b) cluster analysis and (c) volcano plot of the mass spectral features from single ESBL-*E. coli* cells stimulated by CEF for 2 h and 5 h (5 replicates each). (d) The length distribution of single ESBL-*E. coli* cells stimulated by CEF for 2 h and 5 h. The Z-score is measured in terms of standard deviations from the mean, representing the distance between the intensity value of a feature in one cell from the mean intensity value of the feature of all the 10 cells.

Although the bacterial cells with different periods of antibiotic stimulation could be well clustered into two groups, heterogeneous among the bacterial cells with the same period of antibiotic stimulation was observed from the mass spectral features (Figs. 3a and b, Fig. S4 in Supporting information) as well as the cell morphology (Fig. 3d and Fig. S5 in Supporting information). The length of the bacterial cells in the 2 h group varied from 14.1 μm to 42.6 μm; while those in the 5 h group varied from 67.5 μm to 119.7 μm (Fig. 3d). In general, the bacterial cells in the 5 h group were longer than the ones in the 2 h group, which could be on account of the discrimination of the mass spectra features of the two groups.

From the significant features, 11 metabolites were identified by comparing the single cell features to the metabolites identified from a population of ESBL-*E. coli* cells by untargeted metabolomics (Fig. S4 and Data S1 in Supporting information) with MS/MS validation, including ADP-ribose, 3-sulfinylpyruvate, serine, gamma-glu-GABA, proline, L-hydroxyarginine, pantothenate, sorbitol 6-phosphate, dephospho-CoA, histidine and NAD+ (Table S1 in Supporting information). Details about the identification of the features can be found in Supporting information experimental section. All the 11 identified metabolites were labelled in the volcano plot to express their variation tendency visually (Fig. S6 in Supporting information). Except proline and histidine, all the other metabolites in the 5 h group were up-regulated compared to the 2 h group (Fig. 4a). The 11 differential metabolites were then subjected to pathway enrichment using BioCyc. It was found that metabolic changes mainly occurred on amino acid degradation, serine biosynthesis, proline degradation, putrescine degradation, CoA biosynthesis, *etc.*, as shown in Fig. 4b. Amino acids are vital biomolecules for bacterial cells which provide nutrients, control many biological functions and are of great significance in the development of AMR [27]. Putrescine metabolism is relevant to biofilm formation [28] and AMR communication [29]. CoA is an essential cofactor for bacterial cell growth and involved in many metabolic reactions [30]. The fluctuation of these metabolism pathways was due to the disturbance caused by antibiotics.

Yao *et al.* observed that the killing of *E. coli* by beta-lactam antibiotic drugs experiences four steps, *i.e.*, elongation, bulge formation, bulge stagnation and lysis [31]. Nevertheless, metabolic status of bacterial cells with different morphologies is still poorly understood. In order to study the correlation between bacterial cell length and metabolic status, we divided 15 filamentous bacterial cells into five groups on the basis of length, *i.e.*, 0–25 μm, 25–45 μm, 45–60 μm, 60–80 μm, 80–120 μm (Fig. S5 and Table S2 in Supporting information). According to PCA (Fig. 5a), the mass spectral features of the bacterial cells can be well clustered into five discriminative groups in correlation with the bacterial cell length, indicating that the entire metabolic status of ESBL-*E. coli* was perturbed as the length changing. Cluster analysis based on 8 among the 11 metabolites with significant variations between the 2 h and the 5 h groups can divide single bacterial cells into the five groups in terms of length (Fig. 5b), demonstrating that the 8 metabolites were of significance during the bacterial elongation induced by antibiotic stimulation.

Correlation between bacterial cell length and the relative abundance of the 8 metabolites are shown in Fig. 5c and Fig. S7 (Supporting information). The relative abundance of gamma-glu-GABA, 3-sulfinylpyruvate, L-hydroxyarginine and serine were generally up-regulated with the bacterial cell length increasing. When the bacterial cell length reached 80 μm, the relative abundance of gamma-glu-GABA and 3-sulfinylpyruvate kept steady, whereas the relative abundance of L-hydroxyarginine and serine increased continuously. The relative abundance changes of proline and histidine were in an opposite trend, decreasing as the bacterial cell length increasing. In addition, there were also metabolites, *i.e.*, ADP-ribose and sorbitol-6-phosphate, with relative abundance fluctuated during bacterial cell length changing. Their relative abundance increased in the beginning with the bacterial cell length increasing and then declined when the bacterial cell length was larger than 80 μm.

L-Hydroxyarginine, gamma-glu-GABA and proline are metabolites involved in the pathway of arginine and proline metabolism. According to the bacterial pathway knowledge in KEGG, arginine is an amino acid participating in the synthesis of nitric oxide, polyamines, and metabolites of the urea cycle [32]. As shown in Fig. 5d, arginine is the upstream metabolite of L-hydroxyarginine and nitric oxide. Nitric oxide can assist in resisting ROS damage by antibiotics [33]. The persistent increasing of L-hydroxyarginine (Fig. 5c) can be a sign of the increasing production of nitric oxide for anti-ROS damage. In polyamine biosynthesis, arginine is consumed to produce putrescine, which is further converted into gamma-glu-GABA (Fig. 5d). Gamma-glu-GABA is the upstream metabolite of GABA, and GABA is involved in bacterial quorum sensing, which can initiate the formation of resistant subpopulations [34] and is closely associated with biofilm development [35]. The up-regulation of gamma-glu-GABA (Fig. 5c) can demonstrate the activation of GABA biosynthesis for increased biofilm development. In addition, arginine can be transferred to ornithine and further generate proline (Fig. 5d). Proline is a key respiratory substrate of pathogenic bacteria [36]. Antibiotics-based sterilization is often accompanied with accelerated respiration [37], which can explain the decline of proline with bacterial filamentation (Fig. 5c).

Serine and 3-sulfinylpyruvate are metabolites involved in the pathway of cysteine and methionine metabolism that both increased in abundance during bacterial elongation (Fig. 5c). It was reported that cysteine and methionine metabolism is enriched in multi-drug resistant *E. coli* strains compared to drug-sensitive *E. coli* strains [38]. As shown in Fig. 5e, 3-sulfinylpyruvate can be gen-

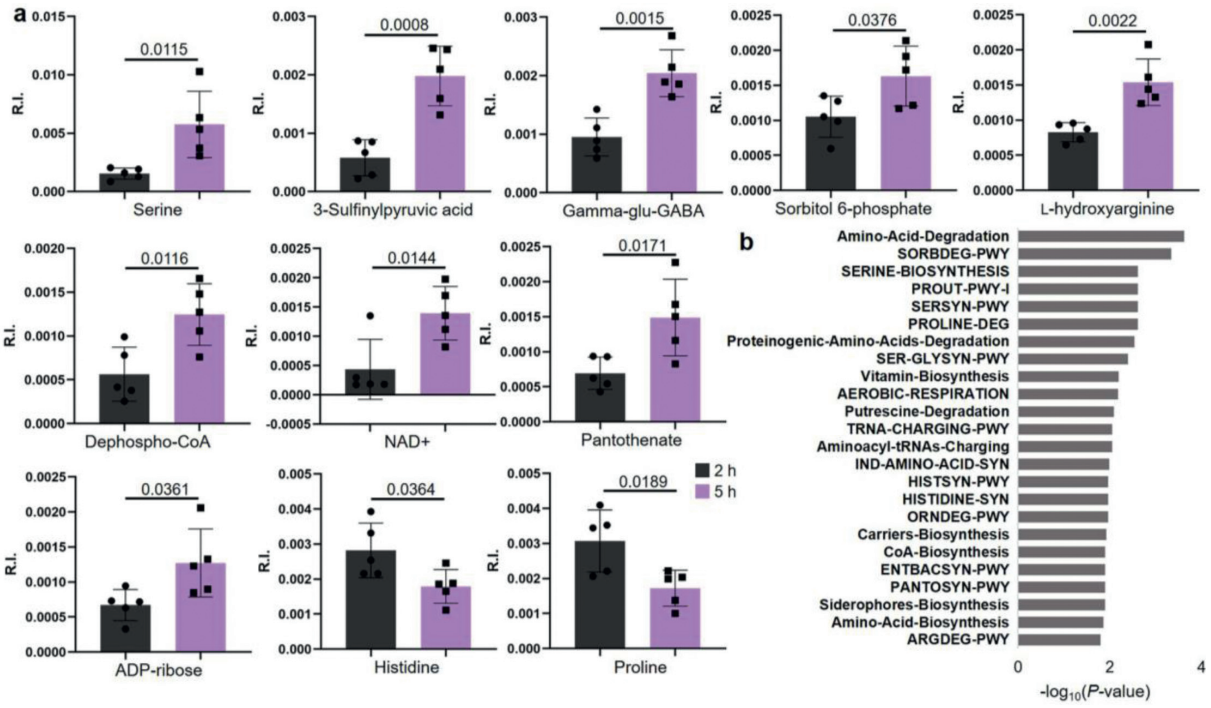

Fig. 4. (a) The relative intensity of metabolites with significant variation in single ESBL-*E. coli* cells between the 2 h group and the 5 h group. Error bars represent the standard derivation ($n = 5$), R.I.: relative intensity. The *P*-value was calculated from T-test. (b) Pathway enrichment of the identified metabolites with significant variations between the 2 h group and the 5 h group. The pathway enrichment was performed by Biocyc.

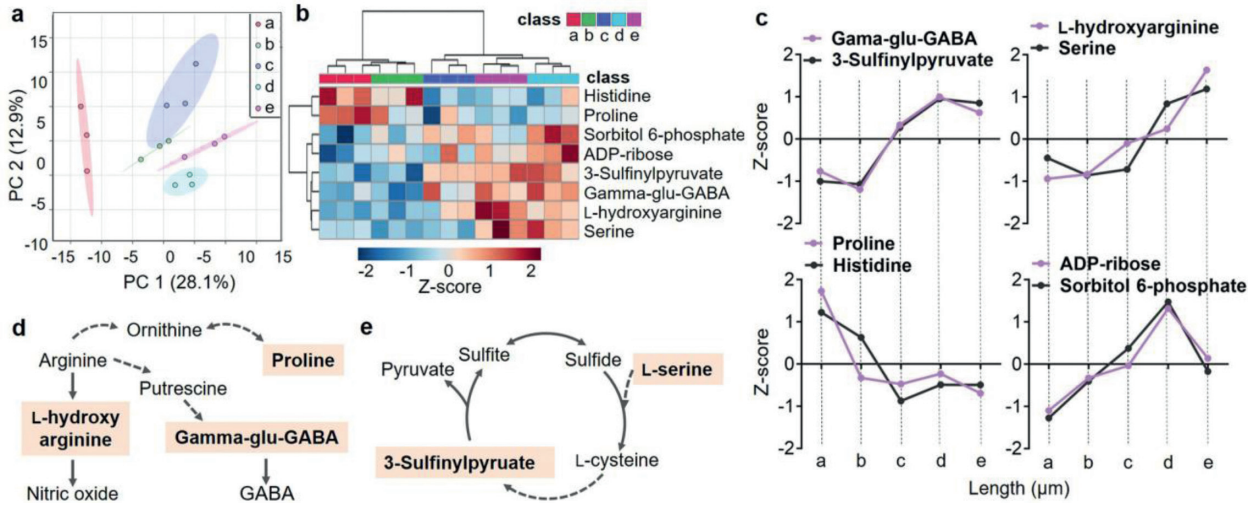

Fig. 5. (a) PCA of mass spectral features of single bacterial cells with different cell length. (b) Cluster analysis based on 8 metabolites to discriminate bacterial cells with varied lengths. (c) Relative metabolite abundance (Z-score averaged from three replicates) variations in correlation with bacterial cell length. Pathways of (d) arginine and proline metabolism and (e) cysteine and methionine metabolism and sulfur metabolism. Bacterial cell length: a, 0–25 μm; b, 25–45 μm; c, 45–60 μm; d, 60–80 μm; e, 80–120 μm. The Z-score represents the distance between the intensity value of a metabolite in one cell from the mean intensity value of the metabolite of all the 15 cells.

erated from L-cysteine through several reactions, and transfer to pyruvate and sulfite. In sulfur metabolism, sulfite turns to sulfide and then converts to L-cysteine in the presence of L-serine. This circular pathway can guarantee cysteine producing continuously. Cysteine is the precursor to produce a number of antioxidant metabolites like glutathione and cofactors, which can assist in resisting ROS damage by antibiotics [39,40]. The up-regulation of serine and 3-sulfinylpyruvate demonstrated the activation of the cysteine production, which can benefit AMR of bacteria [41].

ADP-ribose is the initial metabolite in the pathway of purine metabolism, and involved in the production of adenosine triphosphate (ATP). Sorbitol-6-phosphate is involved in glycolysis [42], which is a vital pathway for energy production [43]. The relative abundance of ADP-ribose and sorbitol-6-phosphate initially increased when ESBL-*E. coli* were stimulated by CEF, and then decreased when the bacterial cell length reached 80 μm (Fig. 5c). Bacterial cells need to produce energy to adjust cell length for survival while need to reduce the oxidative damage from respiratory effect at the same time, and hence fluctuation of energy production related metabolites was observed.

The relative abundance of histidine descended obviously during bacterial filamentation (Fig. 5c), in consistent with the result reported about *Staphylococcus* stimulated by azithromycin [44]. The down-regulation of histidine indicates the activation of histidine

degradation. Glutamate as the end-product of histidine degradation is an important amino acid for glutathione synthesis, while glutathione is an antioxidant to resist ROS damage by antibiotics [45]. The general down regulation of histidine can hence profit bacterial AMR *via* the generation of glutathione.

In summary, we achieved bacterial metabolite detection and analysis of bacterial metabolic regulation during filamentation under the stimulus of antibiotics at single-cell level. Heterogeneous among bacterial cells with the same antibiotic stimulation condition was observed from mass spectra as well as from cell morphology. Eight metabolites, *i.e.*, gamma-glu-GABA, proline, L-hydroxyarginine, serine, 3-sulfinylpyruvate, histidine, ADP-ribose and sorbitol-6-phosphate were found correlating well with the bacteria filamentation by antibiotic stimulation. Pathways, including arginine and proline metabolism, as well as cysteine and methionine metabolism were disclosed closely associated with the bacterial filamentation. Single bacterial cell analysis is more difficult than single-cell analysis due to the low amount of intracellular metabolites in a bacterial cell. In this study, metabolic information obtained by the microprobe ESI-MS is still limited. A large proportion of metabolites are not detected. The future study of single bacterial cell analysis should focus on the improvement of detection sensitivity, such as optimizing lysis method to release more metabolite, and developing more efficient ionization and ion transfer methods as well as mass spectrometry techniques with high sensitivity in metabolites detection.

Declaration of competing interest

The authors declare that they have no known competing financial interests or personal relationships that could have appeared to influence the work reported in this paper.

Acknowledgments

This work was supported by the National Natural Science Foundation of China (NSFC, Nos. 22022401, 22074022 and 21934001), and the Ministry of Science and Technology of China (No. 2020YFF0304502).

Supplementary materials

Supplementary material associated with this article can be found, in the online version, at doi:10.1016/j.cclet.2022.107938.

References

[1] Antiboitic Resistance Threats in the United States CDC Centers for Disease Control and Prevention, Department of Health and Human Services, 2013.
[2] Antibiotic resisance threats in the United States CDC Centers for Disease Control and Prevention, Department of Health and Human Services, 2019.
[3] O. Cars, P. Nordberg, Int. J. Risk. Saf. Med. 17 (2005) 103–110.
[4] B. Peng, H. Li, X. Peng, Expert Rev. Proteomic 16 (2019) 829–839.
[5] S. Aros-Calt, B.H. Muller, S. Boudah, et al., J. Proteome Res. 14 (2015) 4863–4875.
[6] Y. Dai, C. Li, J. Yi, et al., Anal. Chem. 92 (2020) 8051–8057.
[7] R. Pourahmad Jaktaji, S. Pasand, Gene 576 (2016) 115–118.
[8] S.S. Justice, D.A. Hunstad, L. Cegelski, S.J. Hultgren, Nat. Rev. Microbiol. 6 (2008) 162–168.
[9] J. Bos, Q. Zhang, S. Vyawahare, et al., Natl. Acad. Sci. U. S. A. 112 (2015) 178–183.
[10] S. Banerjee, K. Lo, N. Ojkic, et al., Nat. Phys. 17 (2021) 403–409.
[11] C. Giesen, H.A. Wang, D. Schapiro, et al., Nat. Methods 11 (2014) 417–422.
[12] S. Qiu, C. Shen, X. Jian, et al., Chin. Chem. Lett. 33 (2022) 2701–2704.
[13] Z. Wu, L. Lin, Chin. Chem. Lett. 33 (2022) 1752–1756.
[14] S. Xu, M. Liu, Y. Bai, H. Liu, Angew. Chem. Int. Ed. 60 (2021) 1806–1812.
[15] D.H. Mast, H.W. Liao, E.V. Romanova, J.V. Sweedler, Anal. Chem. 93 (2021) 6205–6213.
[16] Q.L. Liu, W.J. Ge, T.T. Wang, et al., Angew. Chem. Int. Ed. 60 (2021) 24534–24542.
[17] C. Wang, W. Hu, L. Guan, et al., Chin. Chem. Lett. 33 (2022) 2883–2892.
[18] X. Gong, Y. Zhao, S. Cai, et al., Anal. Chem. 86 (2014) 3809–3816.
[19] Z. Li, Z. Wang, J. Pan, et al., Anal. Chem. 92 (2020) 10138–10144.
[20] S.J. Standke, D.H. Colby, R.C. Bensen, et al., Anal. Chem. 91 (2019) 1738–1742.
[21] H. Zhu, Q. Li, T. Liao, et al., Nat. Methods 18 (2021) 788–798.
[22] M. Xu, R. Pan, Y. Zhu, et al., Analyst 144 (2019) 954–960.
[23] Y. Zhang, Y. Tang, C. Tan, W. Xu, ACS Central Sci. 6 (2020) 1001–1008.
[24] M. Shehadul Islam, A. Aryasomayajula, P.R Selvaganapathy, Micromachines 8 (2017) 83.
[25] Z. Wei, X. Xiong, C. Guo, et al., Anal. Chem. 87 (2015) 11242–11248.
[26] Waters, Background ion master list, https://www.waters.com/webassets/cms/support/docs/bckgrnd_ion_mstr_lst_4_13_2010.pdf, 2010.
[27] M. Idrees, A.R. Mohammad, N. Karodia, A. Rahman, Antibiotics 9 (2020) 330.
[28] Z. Liu, S. Hossain, Z. Moreira, C. Haney, J. Bacteriol. 204 (2021) e0029721.
[29] O.M. El-Halfawy, M.A. Valvano, Plos One 8 (2013) e68874.
[30] R. Leonardi, S. Jackowski, EcoSal Plus 2 (2007), doi:10.1128/ecosalplus.3.6.3.4.
[31] Z. Yao, D. Kahne, R. Kishony, Mol. Cell 48 (2012) 705–712.
[32] L. Xiong, J.L.L. Teng, M.G. Botelho, et al., Int. J. Mol. Sci. 17 (2016) 363.
[33] I. Gusarov, K. Shatalin, M. Starodubtseva, E. Nudler, Science 325 (2009) 1380–1384.
[34] S.L. Chua, J.K.H. Yam, P.L. Hao, et al., Nat. Commun. 7 (2016) 10750.
[35] C. Solano, M. Echeverz, I. Lasa, Curr. Opin. Microbiol. 18 (2014) 96–104.
[36] S.L. Christgen, D.F. Becker, Antioxid. Redox Signal. 30 (2019) 683–709.
[37] M.A. Lobritz, P. Belenky, C.B. Porter, et al., Natl. Acad. Sci. U. S. A. 112 (2015) 8173–8180.
[38] Y. Lin, W. Li, L. Sun, et al., J. Proteomics 207 (2019) 103468.
[39] G.V. Smirnova, O.N. Oktyabrsky, Biochemistry (Mosc) 70 (2005) 1199–1211.
[40] S.T. Wang, H.W. Chen, L.Y. Sheen, C.K. Lii, J. Nutr. 127 (1997) 2135–2141.
[41] B. Campanini, M. Pieroni, S. Raboni, et al., Curr. Med. Chem. 22 (2015) 187–213.
[42] S. Prasad, P.B. Khadatare, I. Roy, Appl. Environ. Microbiol. 77 (2011) 4603–4609.
[43] W.B. Yu, Q. Pan, B.C. Ye, iScience 21 (2019) 135–144.
[44] W. Ding, Y. Zhou, Q. Qu, et al., Front. Pharmacol. 9 (2018) 740.
[45] M.A.I. Amores-Sánchez, M.Á. Medina, Mol. Genet. Metab. 67 (1999) 100–105.